chemistry proceedings

MDPI

Proceeding Paper

Identification of Quinazoline-Based EGFR Inhibitors Against Triple-Negative Breast Cancer Using an Integrated In Silico Approach †

Faiza Asli

Group of Computational and Medicinal Chemistry, LMCE Laboratory, University Mohamed Khider, Biskra 07000, Algeria; faiza.asli@univ-biskra.dz

† Presented at the 30th International Electronic Conference on Synthetic Organic Chemistry, 5–19 November 2026; Available online: https://sciforum.net/event/ecsoc-30/home.

Abstract

Triple-negative breast cancer (TNBC) is an aggressive subtype lacking ER, PR, and HER2, which limits targeted therapies. Because EGFR is frequently overexpressed in TNBC, quinazoline derivatives were investigated as potential inhibitors using an integrated in silico workflow. Twenty-six compounds were docked against EGFR (PDB ID: 3UG2), followed by MM-GBSA, ADME, and toxicity analyses. Gefitinib showed the strongest predicted binding affinity, while S26, S24, and S16 exhibited distinct computational profiles, with S26 showing the most favorable docking score, S24 the most favorable MM-GBSA binding free energy, and S16 the most favorable predicted toxicity profile. Overall, S24 emerged as the most favorable candidate from a binding and pharmacokinetic perspective, whereas S16 exhibited the most favorable predicted toxicity profile. These findings warrant further experimental validation of the selected compounds.

Keywords: Triple-negative breast cancer; EGFR; Quinazoline derivatives; Molecular docking; MM-GBSA; SwissADME; ProTox-II

1. Introduction

Breast cancer remains the most frequently diagnosed malignancy and a leading cause of cancer-related mortality among women worldwide. More than 2.3 million new cases are diagnosed annually, making it a major public health challenge [1]. Owing to its molecular heterogeneity, breast cancer comprises several subtypes with distinct biological and therapeutic characteristics. Among these, triple-negative breast cancer (TNBC) is one of the most aggressive subtypes, accounting for approximately 15–20% of breast cancer cases [2,3].

TNBC is characterized by the absence of estrogen receptor (ER), progesterone receptor (PR), and human epidermal growth factor receptor 2 (HER2), limiting the use of endocrine and HER2-targeted therapies [4]. Chemotherapy therefore remains an important treatment option; however, its efficacy is often limited by adverse effects, drug resistance, early recurrence, and poor long-term outcomes [3–5]. These limitations highlight the need for effective targeted therapeutic strategies [6].

Among the molecular targets investigated for TNBC, the epidermal growth factor receptor (EGFR) has attracted considerable attention. EGFR is a receptor tyrosine kinase involved in cell proliferation, migration, and survival [7]. Its aberrant activation or overexpression has been associated with poor prognosis, increased metastatic potential, and therapeutic resistance in TNBC [8,9]. EGFR signaling activates pathways such as

Check for updates

Academic Editor: Julio A. Seijas

Published: 14 October 2026

Copyright: © 2026 by the author. Licensee MDPI, Basel, Switzerland. This article is an open access article distributed under the terms and conditions of the Creative Commons Attribution (CC BY) license.

RAS/RAF/MEK/ERK, PI3K/AKT/mTOR, and JAK/STAT, contributing to tumor progression [7,9].

Several EGFR tyrosine kinase inhibitors (TKIs), including Gefitinib, Erlotinib, Afatinib, and Osimertinib, have demonstrated clinical efficacy, particularly in EGFR-mutated non-small cell lung cancer. However, their therapeutic benefit in TNBC has been comparatively limited because of the molecular complexity and resistance mechanisms associated with this disease [10,11]. These limitations have encouraged the development of novel EGFR inhibitors with improved pharmacological properties.

Quinazoline is a privileged scaffold in medicinal chemistry and forms the structural basis of several clinically approved EGFR inhibitors [12]. Its structural versatility allows the development of derivatives with optimized biological activity and target interactions, making quinazoline-based compounds attractive candidates for anticancer drug discovery [13,14].

Computer-aided drug design (CADD) approaches, including molecular docking, binding free energy calculations, pharmacokinetic prediction, and toxicity assessment, facilitate the prioritization of promising compounds before experimental validation [15]. Molecular docking predicts ligand binding modes, while Prime MM-GBSA provides an additional energetic assessment of ligand–protein binding. SwissADME and ProTox-II further support the evaluation of pharmacokinetic and toxicological properties [16–19].

In the present study, an integrated in silico strategy was applied to twenty-six quinazoline derivatives to identify potential EGFR inhibitors against TNBC. The compounds were evaluated using hierarchical HTVS, SP, and XP docking against EGFR (PDB ID: 3UG2), followed by ligand–protein interaction analysis, Prime MM-GBSA calculations, SwissADME, and ProTox-II assessments. This workflow aimed to identify promising derivatives with favorable binding, pharmacokinetic, and predicted safety profiles for further experimental investigation.

2. Materials and Methods

2.1. Dataset Preparation

A dataset comprising twenty-six quinazoline derivatives previously synthesized and evaluated for their antiproliferative activity against the human triple-negative breast cancer cell line MDA-MB-231 was collected from the literature [12]. The experimental IC_{50} values were converted into pIC_{50} values using the following equation:

$$\mathrm{pIC50} = -log10\ (\mathrm{IC50} \times 10^{-6}) \quad (1)$$

The two-dimensional chemical structures were manually drawn using ChemDraw Ultra 16.0 and subsequently converted into three-dimensional structures using Schrödinger Maestro v12.5.

2.2. Ligand Preparation

The 2D chemical structures of the twenty-six quinazoline derivatives were drawn using ChemDraw Ultra 16.0. LigPrep (version 12.5, Schrödinger Release 2020-3) was then used to generate the 3D structures and perform geometry optimization using the OPLS_2005 force field. Possible ionization states at physiological pH (7.0 ± 2.0) were generated using Epik (version 5.5, Schrödinger Release 2020-3), while the original stereochemistry of the compounds was retained. Subsequently, Phase (version 4.6, Schrödinger Release 2020-3) was employed to generate a flexible ligand alignment using the most active compound as the reference template. The prepared ligand structures are provided in Table S1.

2.3. Protein Preparation

The crystallographic structure of the epidermal growth factor receptor (EGFR) kinase domain in complex with Gefitinib (PDB ID: 3UG2) was retrieved from the Protein Data Bank (https://www.rcsb.org). The protein structure was prepared using the Protein Preparation Wizard of Schrödinger Maestro v12.5. Water molecules located beyond the active site were removed, missing hydrogen atoms were added, bond orders were assigned, protonation states were optimized, and restrained energy minimization was performed using the OPLS_2005 force field until convergence.

2.4. Receptor Grid Generation

The receptor grid was generated using the Glide Receptor Grid Generation module implemented in Schrödinger Maestro v12.5 (Schrödinger, LLC, New York, NY, USA). The binding site was defined based on the position of the co-crystallized ligand (Gefitinib) in the crystal structure of EGFR (PDB ID: 3UG2). The receptor grid was centered at X = 0.41, Y = 48.79, and Z = 19.15. The inner docking box was set to 10 × 10 × 10 Å, while the ligand diameter midpoint box (outer box) was configured to 20 × 20 × 20 Å. All remaining grid generation parameters were kept at their default values. as shown in Figure 1.

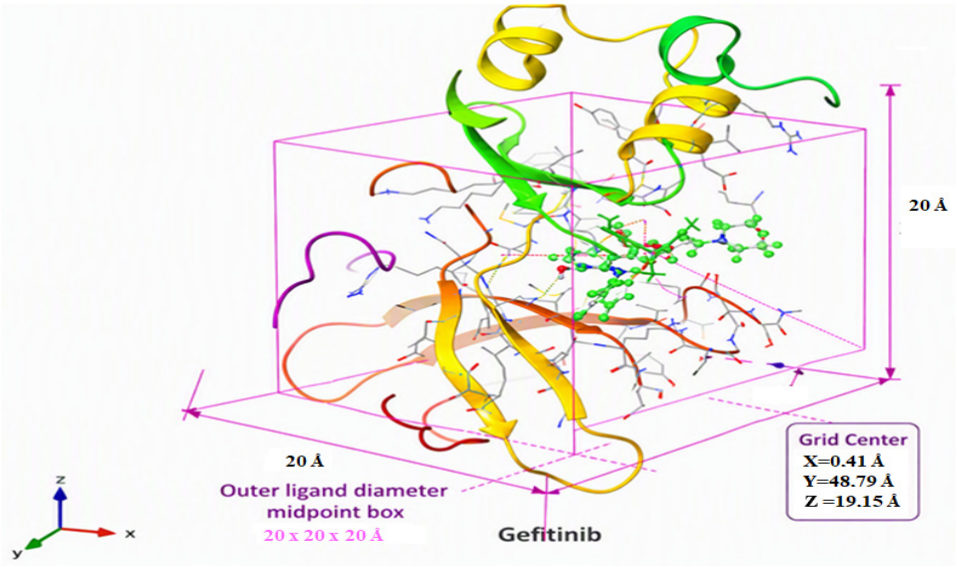


Figure 1. Receptor grid generated for molecular docking of the EGFR tyrosine kinase domain (PDB ID: 3UG2).

2.5. Molecular Docking

Molecular docking was performed using the Glide module implemented in Schrödinger Maestro v12.5 (Schrödinger, LLC, New York, NY, USA). The prepared quinazoline derivatives were docked into the ATP-binding pocket of the epidermal growth factor receptor (EGFR, PDB ID: 3UG2). Initially, all ligands were screened using the High Throughput Virtual Screening (HTVS) protocol. The top-ranked compounds were subsequently subjected to Standard Precision (SP) docking, followed by Extra Precision (XP) docking to obtain a more reliable evaluation of ligand–protein binding affinity.

The co-crystallized ligand, Gefitinib, was prepared separately and re-docked into the active site of EGFR (PDB ID: 3UG2) under the same docking conditions to validate the docking protocol and to serve as the reference ligand. The binding affinities were assessed based on the GlideScore (kcal/mol), and the binding poses together with the ligand–protein interactions were analyzed using the Maestro visualization tools.

2.6. MM-GBSA Binding Free Energy Calculation

Binding free energies of the top-ranked ligand–EGFR complexes were calculated using the Prime MM-GBSA module in Schrödinger Maestro v12.5 with the OPLS_2005 force field and VSGB implicit solvation model. The binding free energy (ΔG_bind) was calculated as:

$$\Delta Gbind = Gcomplex - (Gprotein + Gligand)$$

where Gcomplex, Gprotein, and Gligand represent the energies of the complex, isolated protein, and isolated ligand, respectively. More negative ΔG_bind values indicate more favorable predicted binding.

2.7. Pharmacokinetic (ADME) Prediction

The pharmacokinetic properties of the selected quinazoline derivatives were predicted using the SwissADME web server. The evaluated parameters included physicochemical properties, lipophilicity (LogP), water solubility, gastrointestinal (GI) absorption, blood–brain barrier (BBB) permeability, P-glycoprotein (P-gp) substrate prediction, bioavailability score, drug-likeness according to Lipinski, Ghose, Veber, Egan, and Muegge rules, as well as medicinal chemistry filters including PAINS, Brenk alerts, lead-likeness, and synthetic accessibility.

2.8. Toxicity Prediction

The toxicity profiles of the selected compounds were predicted using the ProTox-II web server. The evaluated parameters included the predicted oral median lethal dose (LD_{50}, mg/kg), toxicity class, hepatotoxicity, carcinogenicity, mutagenicity, immunotoxicity, cytotoxicity, blood–brain barrier (BBB) permeability, and cytochrome P450 (CYP) isoenzyme interactions. These predictions were used to provide a preliminary assessment of the safety profiles of the investigated compounds.

3. Results and Discussion

3.1. Molecular Docking Analysis

To investigate the binding of the synthesized quinazoline derivatives toward the epidermal growth factor receptor (EGFR, PDB ID: 3UG2), a hierarchical molecular docking workflow was performed using the Glide module in Schrödinger Maestro v12.5. The compounds were sequentially screened using High Throughput Virtual Screening (HTVS), Standard Precision (SP), and Extra Precision (XP) docking protocols. The co-crystallized ligand Gefitinib was re-docked under the same conditions and used as the reference ligand.

The docking results are summarized in Table 1. Gefitinib exhibited the most favorable XP GlideScore (−7.780 kcal/mol), whereas S26 showed the best docking score among the investigated derivatives (−7.304 kcal/mol), followed by S16 (−6.842 kcal/mol) and S24 (−6.757 kcal/mol). Other highly ranked derivatives included S4 (−6.506 kcal/mol), S3 (−6.475 kcal/mol), S21 (−6.413 kcal/mol), S1 (−6.399 kcal/mol), S7 (−6.364 kcal/mol), S25 (−6.232 kcal/mol), and S11 (−6.146 kcal/mol).

Overall, the selected derivatives showed favorable predicted binding within the EGFR ATP-binding pocket, although none achieved a more favorable XP GlideScore than Gefitinib. Based on their docking performance and ranking, S26, S24, and S16 were selected for subsequent ligand–protein interaction analysis, Prime MM-GBSA calculations, ADME prediction, and toxicity assessment.

Table 1. Molecular docking results of the reference ligand (Gefitinib) and the top ten quinazoline derivatives against EGFR (PDB ID: 3UG2).

Compound	HTVS GlideScore [1]	SP GlideScore [1]	XP GlideScore [1]	MMGBSA dG Bind [1]
Gefitinib(L_Ref)	−5.163	−5.572	−7.780	−86.34
S_26	−6.776	−7.391	−7.304	−64.99
S_16	−6.672	−7.084	−6.842	−71.83
S_24	−6.558	−7.028	−6.757	−76.85
S_4	−6.297	−6.826	−6.506	−65.64
S_3	−5.909	−6.814	−6.475	−56.72
S_21	−5.748	−6.811	−6.413	−66.80
S_1	−5.640	−6.762	−6.399	−59.96
S_7	−5.543	−6.603	−6.364	−59.81
S_25	−5.476	−6.558	−6.232	−52.02

[1] All GlideScores and MMGBSA ΔG Bind values are expressed in kcal/mol.

3.2. Ligand–Protein Interaction Analysis

The binding modes of S26, S24, and S16 were compared with that of the reference ligand Gefitinib using two-dimensional interaction diagrams generated in Maestro (Figure 2). Gefitinib formed a hydrogen bond with the hinge residue Met793, together with hydrophobic and polar interactions within the EGFR ATP-binding pocket. As summarized in Table S2, all three selected derivatives maintained the conserved hydrogen-bond interaction with Met793.

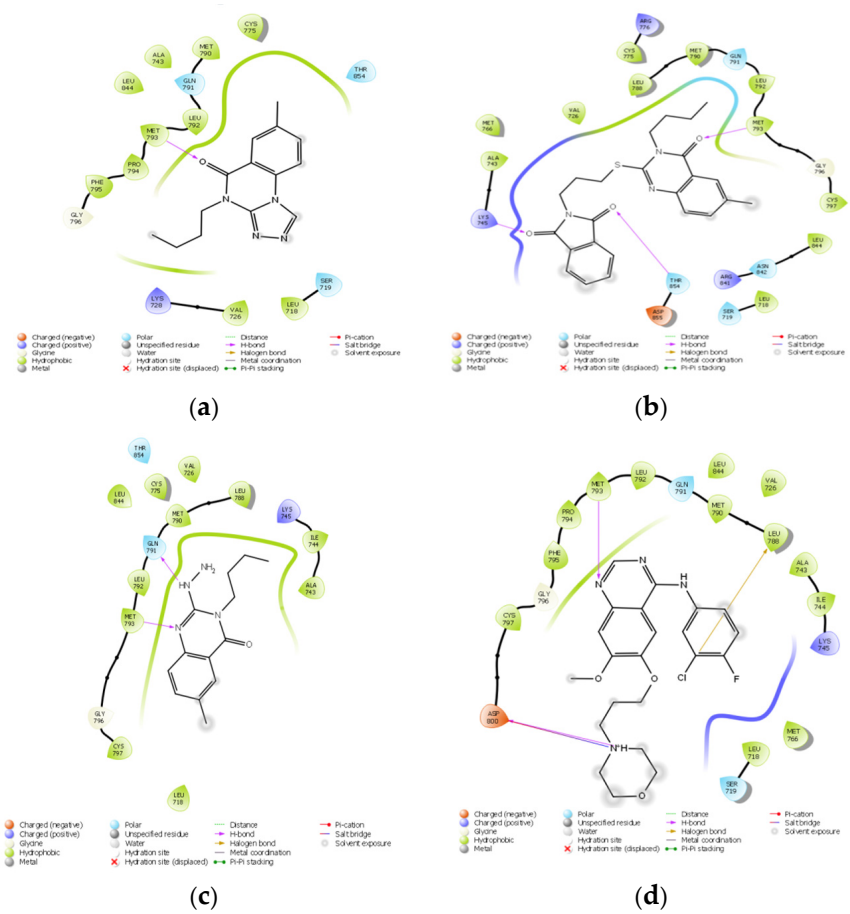


Figure 2. Two-dimensional ligand–protein interaction diagrams of the selected quinazoline derivatives (S26 (**a**), S24 (**b**), and S16 (**c**)) and the reference ligand Gefitinib (**d**) in the ATP-binding pocket of EGFR (PDB ID: 3UG2).

All three selected derivatives maintained the conserved hydrogen-bond interaction with Met793. S26 showed a binding pattern comparable to Gefitinib, with additional hydrophobic and polar contacts. S24 formed two hydrogen bonds with Met793 and Gln791, together with several hydrophobic interactions, consistent with its favorable predicted binding free energy (ΔG_bind = −76.85 kcal/mol). S16 exhibited two hydrogen bonds with Met793 and Thr854, accompanied by extensive hydrophobic, polar, and electrostatic interactions. Overall, the interaction analysis supported the predicted favorable binding modes of the three selected derivatives within the EGFR ATP-binding pocket.

3.3. MM-GBSA Binding Free Energy Analysis

Prime MM-GBSA calculations were performed for the selected ligand–EGFR complexes, and the predicted binding free energies (ΔG_bind) are summarized in Table 2. Gefitinib exhibited the most favorable predicted ΔG_bind (−86.34 kcal/mol), followed by S24 (−76.85 kcal/mol), S16 (−71.83 kcal/mol), and S26 (−64.99 kcal/mol).

Table 2. Prime MM-GBSA binding free energies (ΔG_bind) of the selected quinazoline derivatives and the reference ligand against EGFR (PDB ID: 3UG2).

Compound	XP GlideScore [1]	ΔG_bind [1]
Gefitinib	−7.780	−86.34
S26	−7.304	−64.99
S24	−6.757	−76.85
S16	−6.842	−71.83

[1] All values are expressed in kcal/mol.

Although S26 showed the best docking score among the investigated derivatives (XP GlideScore = −7.304 kcal/mol), S24 exhibited a more favorable predicted MM-GBSA binding energy. This result highlights differences between docking-based scoring and MM-GBSA energetic estimates. The favorable ΔG_bind of S24 is consistent with its multiple hydrogen-bond and hydrophobic interactions within the EGFR binding pocket. Overall, S24 showed the most favorable predicted binding energetics among the investigated derivatives, supporting its selection for further investigation.

3.4. Pharmacokinetic (ADME) Analysis

The pharmacokinetic and drug-likeness properties of S26, S24, and S16 were evaluated using the SwissADME web server and compared with Gefitinib (Table 3). All compounds showed high predicted gastrointestinal absorption, complied with Lipinski's rule of five, and had a bioavailability score of 0.55. The selected derivatives exhibited consensus LogP values ranging from 1.59 to 3.92, with S24 showing the lowest lipophilicity (LogP = 1.59) and the most favorable predicted solubility. S26 was predicted to penetrate the BBB, whereas S24 and S16 were predicted to be non-permeant. No PAINS alerts were identified, while S24 and S16 showed one Brenk alert each. Overall, S24 exhibited the most favorable predicted ADME profile among the selected derivatives.

Table 3. Predicted physicochemical, pharmacokinetic, and drug-likeness properties of the selected quinazoline derivatives and the reference ligand using SwissADME.

Compound	MW	LogP	TPSA (Å^2)	GI Absorption	BBB	Lipinski	Bioavailability	PAINS	Brenk
Gefitinib	447.91	2.64	69.94	High	Yes	Yes	0.55	0	0
S26	256.30	1.84	52.19	High	Yes	Yes	0.55	0	0
S24	246.31	1.59	72.94	High	No	Yes	0.55	0	1
S16	435.54	3.92	97.57	High	No	Yes	0.55	0	1

3.5. Prediction of Toxicity

The toxicity profiles of S26, S24, and S16 were predicted using the ProTox-II web server, and the results are summarized in Table 4. S16 showed the most favorable predicted toxicity profile, with an LD_{50} of 1000 mg/kg (toxicity class 4) and inactive predictions for hepatotoxicity, carcinogenicity, mutagenicity, immunotoxicity, and cytotoxicity. S24 exhibited an LD_{50} of 438 mg/kg (class 4) but showed positive predictions for carcinogenicity and mutagenicity. S26 showed the lowest predicted LD_{50} (255 mg/kg; class 3) and was also predicted to be carcinogenic and mutagenic. Gefitinib showed the highest predicted LD_{50} (2935 mg/kg; class 5), although hepatotoxicity, immunotoxicity, and mutagenicity were predicted. Overall, S16 exhibited the most favorable predicted safety profile, whereas the predictions for S24 and S26 warrant further experimental toxicological evaluation.

Table 4. Predicted toxicity profiles of the selected quinazoline derivatives and the reference ligand using ProTox-II.

Compound	LD_{50} (mg/kg)	Toxicity Class	Hepatotoxicity	Carcinogenicity	Mutagenicity	Immunotoxicity	Bioavailability	Cytotoxicity
Gefitinib	2935	5	Active	Inactive	Active	Active	Inactive	Active
S26	255	3	Inactive	Active	Active	Inactive	Inactive	Inactive
S24	438	4	Inactive	Active	Active	Inactive	Inactive	Inactive
S16	1000	4	Inactive	Inactive	Inactive	Inactive	Inactive	Inactive

4. Conclusions

In the present study, an integrated in silico workflow combining molecular docking, Prime MM-GBSA, ADME, and toxicity prediction was applied to investigate quinazoline derivatives as potential EGFR inhibitors for triple-negative breast cancer (TNBC). Among the investigated compounds, S26 showed the most favorable docking score (XP GlideScore = −7.304 kcal/mol), whereas S24 exhibited the most favorable predicted MM-GBSA binding free energy (ΔG_bind = −76.85 kcal/mol) and a favorable ADME profile. S16 showed the most favorable predicted toxicity profile. All three selected compounds maintained key interactions within the EGFR ATP-binding pocket, including the conserved hydrogen bond with Met793. Overall, S24 represents a promising candidate from a binding and ADME perspective, although its predicted carcinogenicity and mutagenicity warrant further investigation. These computational findings require experimental validation through enzymatic, cellular, and in vivo studies.

Supplementary Materials: The following supporting information can be downloaded at https://www.mdpi.com/article/10.3390/chemproc2026022011/s1, Table S1. Chemical structure and pIC50 values of the investigated quinazoline derivatives; Table S2. Key residue interactions of the selected quinazoline derivatives and the reference ligand within the EGFR active site (PDB ID: 3UG2).

Funding: This research received no external funding.

Institutional Review Board Statement: Not applicable.

Informed Consent Statement: Not applicable.

Data Availability Statement: All data generated or analyzed during this study are included in this published article and its supplementary information files.

Conflicts of Interest: The author declares no conflict of interest.

References

1. Sung, H.; Ferlay, J.; Siegel, R.L.; Laversanne, M.; Soerjomataram, I.; Jemal, A.; Bray, F. Global cancer statistics 2020: GLOBOCAN estimates of incidence and mortality worldwide. *CA Cancer J. Clin.* **2021**, *71*, 209–249. [CrossRef] [PubMed]

2. Bianchini, G.; Balko, J.M.; Mayer, I.A.; Sanders, M.E.; Gianni, L. Triple-negative breast cancer: Challenges and opportunities of a heterogeneous disease. *Nat. Rev. Clin. Oncol.* **2016**, *13*, 674–690. [CrossRef] [PubMed]
3. Waks, A.G.; Winer, E.P. Breast cancer treatment: A review. *JAMA* **2019**, *321*, 288–300. [CrossRef] [PubMed]
4. Foulkes, W.D.; Smith, I.E.; Reis-Filho, J.S. Triple-negative breast cancer. *N. Engl. J. Med.* **2010**, *363*, 1938–1948. [CrossRef] [PubMed]
5. Denkert, C.; Liedtke, C.; Tutt, A.; von Minckwitz, G. Molecular alterations in triple-negative breast cancer—the road to new treatment strategies. *Lancet* **2017**, *389*, 2430–2442. [CrossRef] [PubMed]
6. Garrido-Castro, A.C.; Lin, N.U.; Polyak, K. Insights into molecular classifications of triple-negative breast cancer. *Nat. Rev. Clin. Oncol.* **2019**, *16*, 569–585.
7. Yarden, Y.; Pines, G. The ERBB network: At last, cancer therapy meets systems biology. *Nat. Rev. Cancer* **2012**, *12*, 553–563. [CrossRef] [PubMed]
8. Roskoski, R., Jr. The ErbB/HER family of protein-tyrosine kinases and cancer. *Pharmacol. Res.* **2019**, *139*, 395–411. [CrossRef] [PubMed]
9. Sigismund, S.; Avanzato, D.; Lanzetti, L. Emerging functions of the EGFR in cancer. *Mol. Oncol.* **2018**, *12*, 3–20. [CrossRef] [PubMed]
10. Barker, A.J.; Gibson, K.H.; Grundy, W.; Godfrey, A.; Barlow, J.J.; Healy, M.P.; Woodburn, J.R.; Ashton, S.E.; Curry, B.J.; Scarlett, L.; et al. Studies leading to the identification of ZD1839 (Gefitinib), an orally active EGFR tyrosine kinase inhibitor. *Bioorg. Med. Chem. Lett.* **2001**, *11*, 1911–1914. [CrossRef] [PubMed]
11. Ciardiello, F.; Tortora, G. EGFR antagonists in cancer treatment. *N. Engl. J. Med.* **2008**, *358*, 1160–1174. Correction in *N. Engl. J. Med.* **2009**, *360*, 1579. [CrossRef] [PubMed]
12. Abuelizz, H.A.; Marzouk, M.; Ghabbour, H.A.; Al-Salahi, R. Synthesis and Anticancer Activity of New Quinazoline Derivatives. *Saudi Pharm. J.* **2017**, *25*, 1047–1054. [CrossRef] [PubMed]
13. Antoniolli, G.; Lima, C.S.P.; Coelho, F. Recent advances in the investigation of the quinazoline nucleus and derivatives with potential anticancer activities. *Future Med. Chem.* **2025**, *17*, 1193–1211. [CrossRef] [PubMed]
14. Kaur, J.; Kaur, S.; Anand, A.; Islam, N.; Singh, S.; Singh, A. An Updated Overview on the Synthesis and Anticancer Evaluation of Quinazoline Derivatives. *Chem. Sel.* **2023**, *8*, e202302778. [CrossRef]
15. Sliwoski, G.; Kothiwale, S.; Meiler, J.; Lowe, E.W., Jr. Computational methods in drug discovery. *Pharmacol. Rev.* **2014**, *66*, 334–395. [CrossRef] [PubMed]
16. Friesner, R.A.; Banks, J.L.; Murphy, R.B.; Halgren, T.A.; Klicic, J.J.; Mainz, D.T.; Repasky, M.P.; Knoll, E.H.; Shelley, M.; Perry, J.K.; et al. Glide: A new approach for rapid, accurate docking and scoring. 1. Method and assessment of docking accuracy. *J. Med. Chem.* **2004**, *47*, 1739–1749. [CrossRef] [PubMed]
17. Genheden, S.; Ryde, U. The MM/PBSA and MM/GBSA methods to estimate ligand-binding affinities. *Expert Opin. Drug Discov.* **2015**, *10*, 449–461. [CrossRef] [PubMed]
18. Daina, A.; Michielin, O.; Zoete, V. SwissADME: A free web tool to evaluate pharmacokinetics, drug-likeness and medicinal chemistry friendliness of small molecules. *Sci. Rep.* **2017**, *7*, 42717. [CrossRef] [PubMed]
19. Banerjee, P.; Eckert, A.O.; Schrey, A.K.; Preissner, R. ProTox-II: A webserver for the prediction of toxicity of chemicals. *Nucleic Acids Res.* **2018**, *46*, W257–W263. [CrossRef] [PubMed]

Disclaimer/Publisher's Note: The statements, opinions and data contained in all publications are solely those of the individual author(s) and contributor(s) and not of MDPI and/or the editor(s). MDPI and/or the editor(s) disclaim responsibility for any injury to people or property resulting from any ideas, methods, instructions or products referred to in the content.